Physics Today

Vortices in Rotating Superfluid He 3

Pertti Hakonen and Olli V. Lounasmaa

Citation: Physics Today **40**(2), 70 (1987); doi: 10.1063/1.881100
View online: http://dx.doi.org/10.1063/1.881100
View Table of Contents:
http://scitation.aip.org/content/aip/magazine/physicstoday/40/2?ver=pdfcov
Published by the AIP Publishing

Vortices in rotating superfluid He^3

Completely novel continuous vortices in He^3-A and spontaneously magnetized singular vortices in He^3-B are just two of the many interesting peculiarities of rotating superfluid He^3.

Pertti Hakonen and Olli V. Lounasmaa

For about a century now, physicists have been working hard to extend the temperature range accessible to experimental investigations closer and closer to absolute zero. This endeavor has been amply rewarded by new and fundamentally important discoveries.

Thus, for example, it was long believed that helium-4 was unique in supporting a superfluid phase, because it consists of bosons and its atoms are sufficiently light that it remains liquid at absolute zero. However, in 1972, Douglas Osheroff, Robert Richardson and David Lee, working at Cornell University, found that helium-3, which is a fermion system, is a superfluid at temperatures below 3 mK, and that in fact there are two distinct phases of the superfluid, He^3-A and He^3-B. Their paper started a new and exciting era in ultralow-temperature physics.

As William Glaberson and Klaus Schwarz explain in their article on page 54, rotating a superfluid creates a regular vortex array in the fluid. In 1982 our group at the Helsinki University of Technology built a rotating cryostat (figure 1) and began to investigate experimentally vortices in rotating superfluid He^3. We have uncovered many surprising phenomena. For example, the A phase supports a continuous distribution of vorticity, like a normal liquid, but the texture is like that of a liquid crystal; this structure is forbidden in a "classical" superfluid such as He^4-II. He^3-B exhibits a vortex-core phase transition and a gyromagnetic effect; experimental data show that the vortex cores have a spontaneous magnetic moment. Figure 2 illustrates the phase diagram of He^3.

Because the He^3 nucleus—unlike that of He^4—has a magnetic moment, it is possible to use nuclear magnetic resonance to study the behavior of superfluid He^3. Our nmr studies have played a decisive role in experimental research on rotating liquid He^3 at millikelvin temperatures. But because He^3 is a complicated system, considerable theoretical efforts were needed to explain the observations.

In this article we briefly discuss some of the interesting phenomena associated with rotating superfluid He^3. Readers interested in more details, particularly on the relevant theory, should consult several recent review papers.[1] These also provide more complete lists of references.

Superfluid phases of He^3

Although both He^3 and He^4 are superfluids at sufficiently low temperatures, the superfluidity in He^3 is more closely related to superconductivity than to the superfluidity in He^4, which is a manifestation of a Bose–Einstein condensation. Superfluidity in He^3, on the other hand, is, like superconductivity in metals, the result of a pairing of Fermi–Dirac particles. The Bardeen–Cooper–Schrieffer theory of superconductivity can therefore be adapted to superfluid He^3; this accounts for the rapid theoretical advances in understanding superfluid He^3.

In superconductors the orbital angular momentum L and spin S of the Cooper pairs of conduction electrons are both zero. In He^3 the strong repulsive force exerted by the atomic cores prevents such s-wave pairing; instead, the pairs form an orbital p-wave state, with L and S both equal to 1. The nonzero spin of Cooper pairs in superfluid He^3 produces a magnetic ordering similar to that observed in antiferromagnets. In addition, the nonvanishing orbital angular momentum causes spatial anisotropy in the superfluid; the He^3-A and He^3-B phases resemble liquid crystals with uniaxial and biaxial anisotropy, respectively.

The transition from the normal Fermi liquid to the superfluid phases is a second-order phase transition, whereas the transition between the superfluid phases He^3-A and He^3-B is a first-order transition, involving a latent heat.

The superfluid state can be described by a macroscopic wavefunction $\Psi(\mathbf{r})$, usually called the order parameter. For a p-wave superfluid the order parameter is a 3×3 matrix that reflects the angular momentum state of the system:

$$\Psi_{\alpha\beta}(\mathbf{r}) = \mathscr{A}_{\alpha\beta}(\mathbf{r})e^{i\Phi(\mathbf{r})}$$

The matrix $\mathscr{A}_{\alpha\beta}$ can be expressed in terms of spherical harmonics for the spin (α) and orbital (β) parts. The directions of quantization of $\mathbf{L}$ and $\mathbf{S}$ are not necessarily the same, so the spherical harmonics are referred to different axes; these are denoted by $\hat{l}$ (for $\mathbf{L}$) and $\hat{\zeta}$ (for $\mathbf{S}$). He^3-A is in a state for which $<S_\zeta>$ is 0 and $<L_l>$ is 1, so that only one component, $\mathscr{A}_{01}$, is different from zero. In He^3-B, the total angular momentum J is 0, and there are three nonzero components of the matrix, $\mathscr{A}_{1,-1}$, $\mathscr{A}_{0,0}$ and $\mathscr{A}_{-1,1}$.

In figure 3 we have attempted to clarify the pairing situations in He^3-A and He^3-B; the ground state of a superconductor is included for comparison. Pairing occurs between two He^3 quasiparticles on opposite sides of the Fermi sphere. Of the possible $S=1$ spin substates, $|\uparrow\uparrow\rangle$, $|\downarrow\downarrow\rangle$ and $|\downarrow\uparrow\rangle + |\uparrow\downarrow\rangle$, the strongly anisotropic He^3-A contains only the first two, whereas all the substates are present in He^3-B. In a high magnetic field a third superfluid phase, He^3-A1, appears; in this case

Pertti Hakonen is Senior Scientist in the Low Temperature Laboratory of the Helsinki University of Technology, Espoo, Finland. Olli Lounasmaa is a research professor of the Academy of Finland and director of the Low Temperature Laboratory.

0031-9228 / 87 / 0200-0070 / $01.00

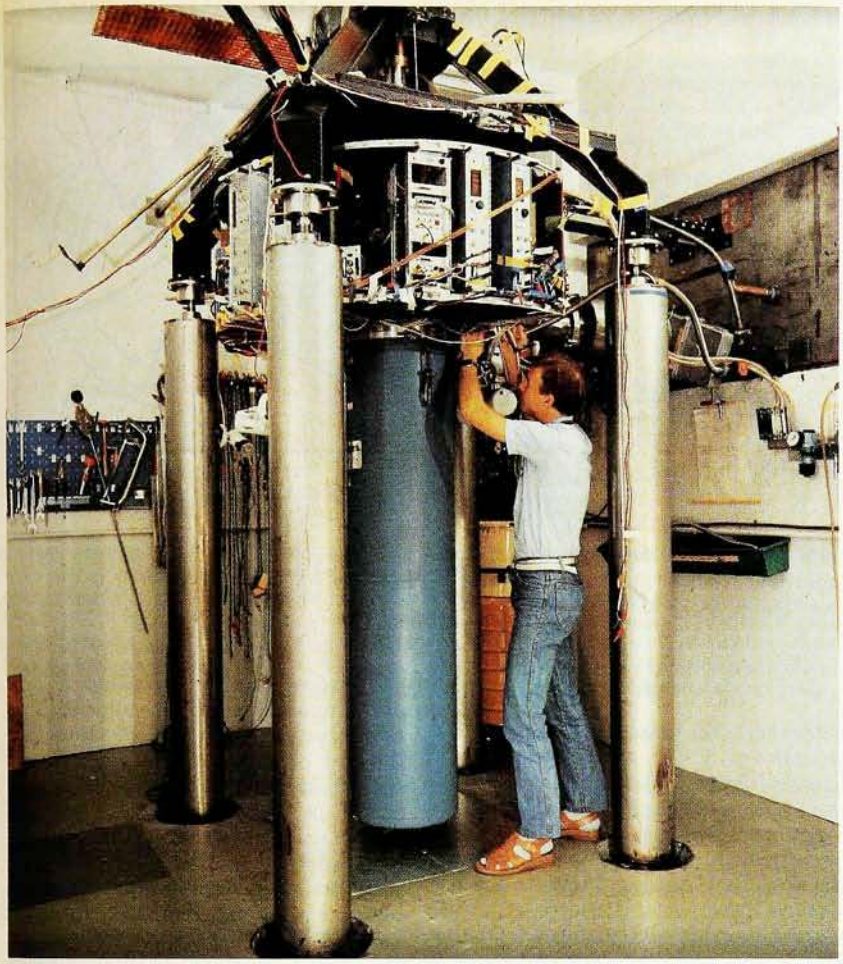

ROTA laboratory at the Helsinki University of Technology in Espoo, Finland. The rotating cryostat is supported on the four pillars at the center of the photo. Graduate student Kaj Nummila is preparing the cryostat for rotation by disconnecting the external pumping lines. Figure 1

only the second spin substate, $|\downarrow\downarrow\rangle$, is populated.

In He^3-A the energy gap $\Delta(T)$ is anisotropic and has nodes in the direction of $\hat{l}$. The Cooper pairs can be considered as ring-shaped "molecules" whose symmetry axis is along the $\hat{l}$ axis. The magnetic anisotropy axis of the liquid is given by a unit vector $\hat{d}$, which is perpendicular to $\hat{\zeta}$ and points, in He^3-A, in the same direction everywhere on the Fermi surface.

As soon as the directions of the $\hat{l}$ and $\hat{d}$ vectors have been specified, the order parameter is fixed except for a phase angle. The two spin populations are paired separately, but the orbital angular momenta of the spin-up and spin-down pairs are all along the same direction $\hat{l}$. The average value of the spin is zero, so there is no spontaneous magnetization. Many properties of He^3-A, for instance viscosity and ion mobility, are different in directions parallel and perpendicular to $\hat{l}$. Hence He^3-A is like an anisotropic superfluid liquid crystal.

The spatial structure of the $\hat{l}$ vector is called a texture; it is determined by competition among several interactions. In He^3-A, the dipolar spin–orbit coupling tends to align the orbital angular momentum axis $\hat{l}$ and the magnetic axis $\hat{d}$, the bending energy tends to straighten the $\hat{l}(\mathbf{r})$ and $\hat{d}(\mathbf{r})$ fields and keep them uniform, the interactions with the walls and the streaming fluid tend to turn $\hat{l}$ perpendicular to the walls and in the direction of the superfluid flow, and the external magnetic field tends to turn $\hat{d}$ perpendicular to the applied field $\mathbf{H}$. The strengths of these orienting effects may conveniently be compared by means of "healing lengths," which give the distance beyond which a particular interaction overcomes the forces tending to keep the $\hat{l}$ and $\hat{d}$ fields uniform.

The spherically symmetric He^3-B is isotropic both in the orbital and in the spin space. Therefore, the $\hat{d}$ and $\hat{l}$ vectors cannot be constant over the Fermi surface. Instead, the ordering is described by a vector $\hat{n}$, which originates from the broken relative rotational symmetry of the spin and orbital spaces, caused by the tiny dipolar interaction of Cooper pairs. This dipole-interaction energy is minimized when the spherically symmetric $\hat{d}$ distribution is rotated locally at each point on the Fermi sphere by 104° about $\hat{n}$. Figure 3 shows the resulting $\hat{d}$ vectors in the equatorial plane of the Fermi surface; at other "latitudes" the angle between $\hat{d}$ and $\hat{n}$ is smaller than 90°. The $\hat{n}$ vector tends to be parallel to $\mathbf{H}$ and its direction is also affected by other interaction forces of the liquid.

In He^3-B the average values of both the spin and the orbital angular momenta of quasiparticle pairs are zero. The texture is fully described by the $\hat{n}$ vector, which in equilibrium defines the axis for the tiny anisotropy of the B phase, in both the spin and the orbital spaces. The anisotropy is smaller than that of the A phase by a factor of 10^5; the B phase can therefore be regarded as an isotropic superfluid. In addition, all orienting forces on the $\hat{n}$ vector are about five orders of magnitude weaker than the corresponding effects on the $\hat{l}$ vector in He^3-A.

Rotating superfluid He^3

For the same reasons as in superfluid He^4, a regular vortex array is formed in uniformly rotating superfluid He^3. Vortices are also generated easily by liquid flow when the superfluid velocity $\mathbf{v}_s$ exceeds a critical value, but in this case a tangled mess of vortices is created. To study orderly vortex textures, one must therefore rotate superfluid He^3 smoothly and uniformly. The typical experimental setup for nmr measurements consists of a cylindrical He^3 cell that can be made to rotate about its (vertical) axis, surrounded by a magnet that can apply a vertical magnetic field.

In superfluid He^4 the order parameter is a scalar quantity, and $\mathbf{v}_s$ is proportional to $\nabla\Phi$, the gradient of the phase of the wavefunction. As a result, the superfluid flow is irrotational ($\nabla\times\nabla\Phi$ vanishes); that is, it satisfies the Landau criterion.

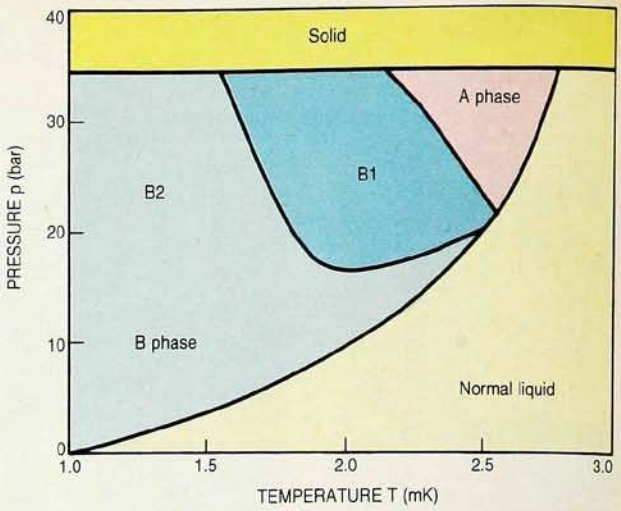

Phase diagram of He^3 below 3 mK. There are two superfluid phases, A and B, and the rotating B phase exhibits a phase transition between two vortex structures, B1 and B2. At a pressure of 21.2 bar and a temperature of 2.55 mK the three liquid phases are in thermal equilibrium with one another. To convert the temperatures given in this article to those of the most recent scale, proposed by Dennis Greywall, multiply our figures by 0.89. Figure 2

In He^3-A the situation is not so simple: It turns out that the A phase can support not only the singular vorticity characteristic of superfluid He^4, but also what is called continuous vorticity in the presence of a spatially varying distribution of the anisotropy axis $\hat{l}$.

A singular vortex has two cores: a "hard" core, whose radius is the coherence length ξ, about 10 nm, inside which the order parameter deviates sharply from its value in bulk He^3-A due to the singularity; and a "soft" core with a radius on the order of the dipolar healing length, $\xi_D{}^A$, about 6 microns. Continuous vortices have only a soft core. In the bulk liquid outside $\xi_D{}^A$, the texture $\hat{l}$ is practically uniform; all vorticity in the superfluid is thus concentrated inside the soft core. Both types of vortices are well localized because the intervortex distance is at least an order of magnitude larger than $\xi_D{}^A$ at all experimentally accessible rotation speeds.

Which vortex texture, singular or continuous, actually forms in He^3-A under rotation depends, according to theory, on the external magnetic field, on the dimensions of the sample and on the angular velocity Ω. Estimates show that when the magnetic field is above 2.5 mT, singular vortices are preferred for angular velocities less than 1 rad/sec; their creation, however, requires overcoming a high potential barrier. As a result, singular vortices are most likely to be formed at the walls, whereas continuous vortices can also be created in the bulk liquid. Therefore continuous vortices may be formed first, and once they exist in metastable states, it becomes difficult to transform one continuous vortex into two singular ones.

David Mermin and Tin-Lun Ho[2] have shown that superflow is coupled to the angular momentum of the Cooper pairs. In particular, the curl of the superflow velocity is, in cylindrical coordinates (r, ϕ and z),

$$(\nabla\times\mathbf{v}_s)_z = \frac{\hbar}{2m_3 r}\,\hat{l}\cdot\left(\frac{\partial\hat{l}}{\partial\phi}\times\frac{\partial\hat{l}}{\partial r}\right) \qquad (1)$$

where m_3 is the mass of a He^3 atom. If $\hat{l}$ is uniform, $\nabla\times\mathbf{v}_s$ vanishes and only singular vortices are created by rotation. When $\hat{l}$ changes its direction as a function of position, continuous vortices may be formed; the fields $\mathbf{v}_s(\mathbf{r})$ and $\hat{l}(\mathbf{r})$ then have no singularities. Figure 4 shows the superfluid velocity of He^3-A as a function of radial distance from the center for singular and continuous vortex distributions in a uniformly rotating cylinder.

The A phase thus rotates in a manner that is intermediate between the ordinary solid-body rotation of a classical liquid and the behavior of superfluid He^4. He^3-A could, in fact, rotate just like a viscous liquid, but this would be costly in the energy of the resulting $\hat{l}$ texture.

Before the discovery of superfluid He^3, the Landau criterion of curl-free flow was considered an essential property of every superfluid. It has now become necessary to revise many theoretical concepts of superfluids, including, in particular, their behavior under rotation. For "traditional" superfluids, the circulation K, taken around any closed contour surrounding a vortex, is an integer multiple of the circulation quantum h/M:

$$K = \oint \mathbf{v}\cdot d\boldsymbol{\sigma} = Nh/M;$$

For He^3 the mass M is $2m_3$ because of Cooper pairing. For continuous vortices, this quantum condition is valid only along the boundary of the primitive cell in the vortex lattice.

In the isotropic He^3-B the superfluid velocity field is determined by the gradient of the phase of the order parameter, as in He^4-II:

$$\mathbf{v}_s = \frac{\hbar}{2m_3}\nabla\Phi$$

The flow is thus irrotational, and only singular vortices are allowed. Prior to experiments, He^3-B was therefore thought of as a rather uninteresting superfluid, but this expectation turned out to be completely wrong. An extended vortex core, about two orders of magnitude larger than in He^4-II, and a peculiar intrinsic coupling between its liquid crystal and magnetic properties make the He^3-B phase vortices intriguing objects of study.

Special textural effects, arising from counterflows of the superfluid and normal components, modify the $\hat{n}(\mathbf{r})$ field in He^3-B. This interaction is strongest immediately after rotation has been started, when the normal liquid is moving with the container, with velocity $\mathbf{v}_n$, but the superfluid is still at rest. When the equilibrium density of vortices has been established and the difference between the normal and superfluid velocities approaches zero, the texture of rotating He^3-B changes due to the influence of vortices on the $\hat{n}$ vector. This orienting effect is produced by the local superflow around vortices and by the vortex cores. Inside the core the magnetic anisotropy, which orients $\hat{n}$, is of the same order of magnitude as in He^3-A—about 10^5 times larger than in bulk He^3-B.

The local superflow also gives rise to a spontaneous magnetic moment of vortex cores. This gyromagnetic effect originates from the rigidity of the quantum state, that is, the tendency to keep the expectation value of the total angular momentum J equal to zero. The orbital angular momentum L is thus compensated by a spin, giving rise to a magnetization. At a rotation speed of 1 rad/sec the magnetization is on the

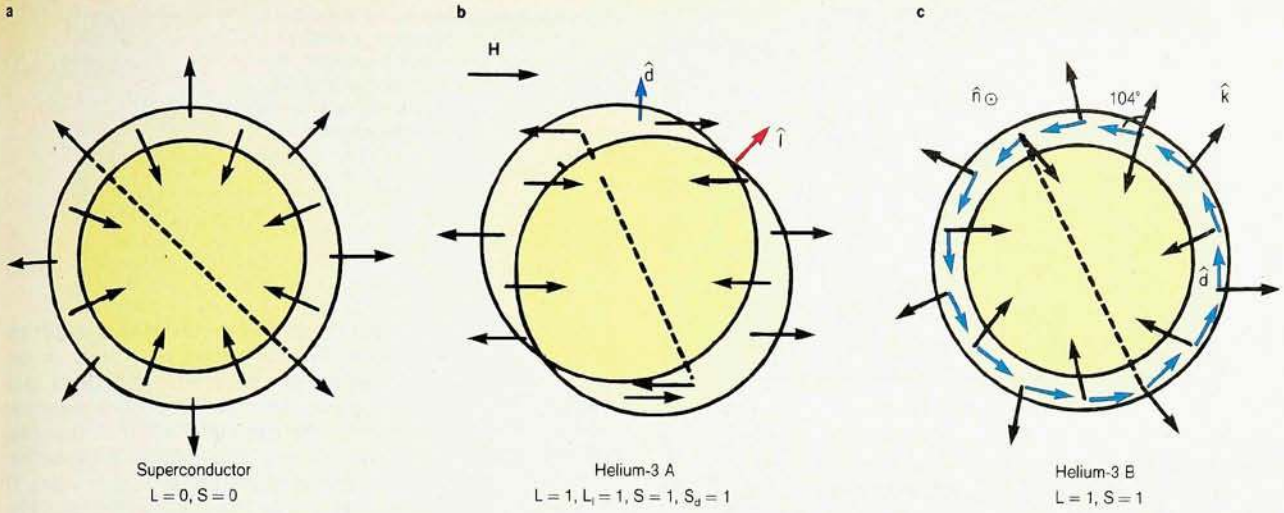

Cooper pairing: The Fermi sphere (yellow) and the energy gap between the paired states and the excited states of unpaired quasiparticles (pale yellow) in wavevector space. Spins are shown as black arrows; dashed lines indicate pairing. **a:** Electrons in a superconductor. The phonon-mediated BCS interaction pairs electrons with opposing spins on opposite sides of the Fermi surface. The pairs form in a singlet ($L = 0, S = 0$) state. **b:** He^3 atoms in the superfluid A-phase. The atom pairs form in an anisotropic triplet state with spins aligned along the magnetic field ***H*** and orbital angular momenta aligned along $\hat{l}$. The vector $\hat{d}$ gives the magnetic anisotropy of the liquid. (This is the Anderson–Brinkman–Morel model of He^3-A.) **c:** He^3 atoms in the superfluid B-phase. The atom pairs form an isotropic triplet state. The vector $\hat{n}$ gives the direction of the anisotropy of the B phase. (This is the Balian–Werthamer model of He^3-B.) Figure 3

order of 10^{-11} nuclear Bohr magnetons per atom of the liquid.

Experimental studies

Most of the experiments on rotating superfluid He^3 have been made in the ROTA minilab at Helsinki; several investigations on the flow properties have been done in John Reppy's laboratory at Cornell University. Figure 1 is a photograph of the ROTA cryostat, which is a joint project of the Academy of Finland and the USSR Academy of Sciences. The rotating part of the apparatus incorporates an experimental He^3 chamber, a copper nuclear demagnetization stage, an 8-T superconducting solenoid, a dilution refrigerator, an activated charcoal cryoadsorption pump, radial and axial air bearings, and computerized measurement electronics.

The nuclear stage was manufactured from a single rod of high-purity copper, 43 mm in diameter and weighing 4.0 kg, with 0.8-mm-wide grooves milled 1.5 mm apart along its length to avoid eddy-current heating during demagnetization. The He^3 chamber is located on top of the nuclear stage and is thermally connected to it by means of very fine sintered silver powder.

During an experiment the copper nuclear stage is first precooled to 18 mK, with the high-field magnet on, by means of the dilution refrigerator, operated by external pumps. The copper rod is then thermally isolated and demagnetized over 10 hours to 150 mT, cooling it to 0.4 mK. Next the dilution refrigerator is switched from circulating to single-cycle mode by disconnecting the external pumping line and starting the charcoal pump. (For details on dilution refrigeration and nuclear cooling, see the article by Lounasmaa in PHYSICS TODAY, December 1979, page 32.)

The cryostat is now ready for rotation; the maximum angular velocity Ω in either direction is 3 rad/sec. The instruments on the rotating platform are connected to their power supply via low-friction carbon-brush slip rings. The measuring signals are first amplified and then fed, in digital form, through an optical data transmission unit to the stationary information acquisition system outside the electrically shielded cryostat room. The same optical coupler is employed as a command channel.

In about 12 hours the He^3 supply in the dilution refrigerator becomes exhausted; the cryostat must then be stopped and connected again to the external pumps. After the charcoal has been regenerated, a new experimental sequence can be started in about 24 hours.

Localized spin waves in He^3-A

One of the most direct probes of the superfluid state is nuclear magnetic resonance. The coherent interaction between quasiparticles leads to big frequency shifts in the nmr spectrum of He^3, shifts that depend on the order parameter.[3] Large structures, such as the vortex cores in He^3-A, have clear effects on the nmr signal. The vortex cores in He^3-B, which are smaller by a factor of a thousand, can nevertheless be observed by nmr through their influence on the overall texture.

The nmr absorption frequency f of stationary superfluid He^3-A is shifted from the Larmor frequency f_0 of normal He^3. Anthony Leggett[4] has shown that the frequency depends on the temperature according to

$$f^2 = {f_0}^2 + \lambda_g {f_A}^2 (1 - T/T_c)$$

where f_A is 2×10^5 Hz. The parameter λ_g describes the texture of the fluid. For a uniform liquid

$$\lambda_g = \cos 2\theta$$

where θ is the angle between the $\hat{d}$ and $\hat{l}$ vectors. For a nonuniform texture, the coherent spin precession within the dipole healing length results in a spin wave of definite frequency, localized at the nonuniformity.

The effect of rotation is to broaden the main nmr line of He^3-A and to create an additional peak. The frequency of the satellite does not change with the angular velocity, but its intensity depends linearly on Ω. This is just the behavior expected for isolated vortices whose number increases proportionally with Ω. Figure 5 shows a typical nmr spectrum of a sample of He^3-A.

The broadening of the main peak is caused by increased spin diffusion and spin-wave scattering due to vortices in the bulk liquid. The satellite is caused by a bound spin-wave mode localized at

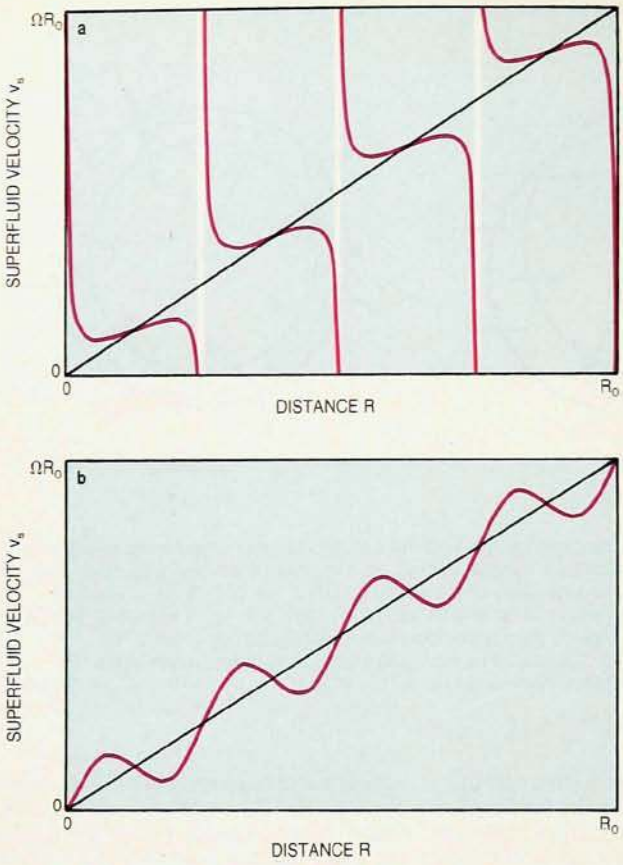

Tangential component of the superfluid velocity field v_s as a function of distance from the center of a rotating cylinder. **a:** Singular vorticity. **b:** Continuous vorticity. The diagonal lines indicate the relationship for a solid body rotating with angular velocity Ω. Figure 4

the vortex core—this spin wave must be large to be able to produce a peak responsible for 10% of the total nmr absorption at 2 rad/sec. The energy of the spin wave can be calculated from the Leggett equations that describe the spin dynamics in superfluid He^3. By comparing the calculated energy of this mode with the measured nmr frequency of the satellite, one can infer the distribution of $\hat{l}$ vectors in the vortex core.

The Leggett equations lead to a Schrödinger equation with a potential determined from the $\hat{l}(\mathbf{r})$ distribution and having a bound state corresponding to a spin wave localized at the vortex core. The bound state is not very sensitive to the detailed shape of the potential; there are several vortex structures with different internal symmetries that produce experimentally indistinguishable energies of the spin wave. The energy of the bound state is, however, very sensitive to the spatial extent of the potential well. The nmr response of the "small," singly quantized, singular vortices, which are energetically favored above 2.5 mT, can thus be easily distinguished from that of the "large," metastable, doubly quantized, continuous vortices that are actually observed.

Experiments indicate that vortices in He^3-A are formed only above a critical rotation velocity, as is the case in He^4-II. The critical velocity depends on the container size—for cylinders of radii 2.5 mm and 0.25 mm, it is about 0.1 rad/sec and 1.0 rad/sec, respectively. In He^3-A, after the critical speed has been exceeded, continuous vortices enter the sample rather quickly—in a few seconds. In He^4, by contrast, the creation of singular vortices may take several minutes.

Behavior of He^3-B

As we have said, the texture of He^3-B is described by the vector $\hat{n}$ determining the axis of the tiny anisotropy of the B phase. In the cylindrical cells we use (about 2.5 mm in diameter), the $\hat{n}$ vector spirals smoothly from a fixed orientation at walls toward the magnetic field **H** along the cylinder axis, forming the so-called flare-out texture. The angle β between $\hat{n}$ and **H** is 0° at the axis and 63° at the walls. This leads to a broad nmr line because the frequency shift is proportional to $\sin^2\beta$.

The spin dynamics for He^3-B leads to an equation analogous to a Schrödinger equation in which $\sin^2\beta$ acts as a potential. The center of the texture thus forms a two-dimensional harmonic potential well that supports localized spin-wave modes with equal spacing in frequency. These can be seen, superimposed on the broad nmr line, in the measured spectra[5]; examples are shown in figure 6. From such measurements one can conclude that the spin-wave spacing increases under rotation; the frequency shift is larger when Ω and **H** are in the same direction. The frequency shift for each line decreases as a function of temperature; for the rotating B phase there is a rather sharp discontinuity at a temperature of $0.6T_c$, with the frequency shift jumping by more than 20%.

Rotation alters the steepness of the $\sin^2\beta$ potential by changing the magnetic healing length ξ_H. The value of the healing length depends on the magnetic properties of the vortex core:

$$\xi_H \approx (1 - \lambda \pm \kappa/H)^{-1/2}$$

The constant κ reflects the spontaneous magnetization of the core, which is thus responsible for the different frequency shifts when the magnetic field is parallel or antiparallel to the rotation. The constant λ describes the susceptibility of the core.

Phase transition. The temperature T_v at which the discontinuity in figure 6 occurs does not depend on **H** or on Ω. Both λ and κ, as obtained from the data on spin-wave spacing, are discontinuous at T_v. The discontinuity Δf must therefore be due to a structural reordering in the vortex cores. We observed superheating across this discontinuity, so a first-order phase transition must be involved.

Under rotation the B phase thus splits into two regions, B1 and B2, with different vortex structures. The temperature T_v of the transition between the two vortex structures depends on the pressure, and we have been able to map much of the curve that separates the regions B1 and B2, using measurements made at magnetic fields of 28 and 57 mT (see figure 2). Because the frequency shifts Δf diminish near T_c, it is experimentally difficult to determine T_v close to T_c. However, a linear extrapolation suggests that the T_v curve hits the superfluid–normal-liquid boundary slightly below the polycritical point, where the normal, A and B2 phases are in equilibrium. A first-order phase boundary could also end

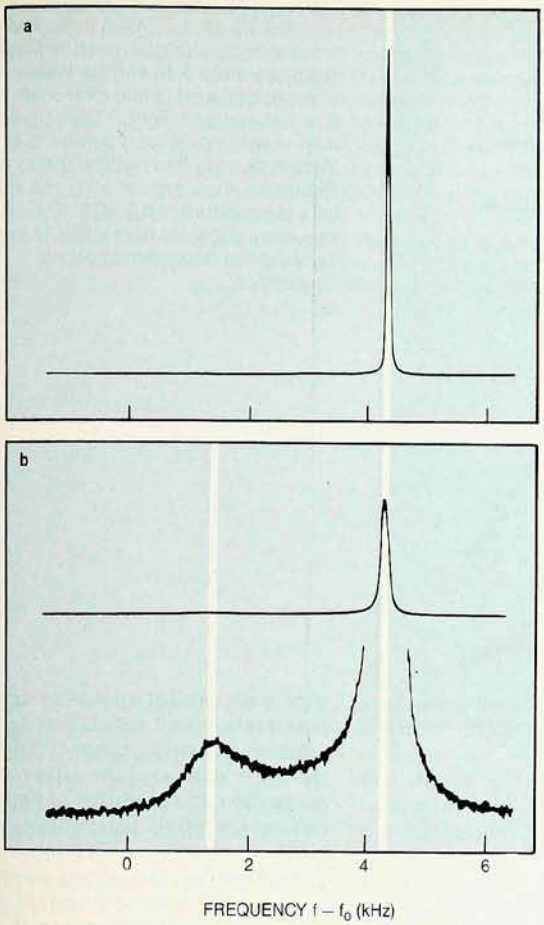

Transverse nmr absorption in He^3-A at a temperature of $0.73T_c$ and pressure of 29.3 bar in an axial magnetic field of 28.4 mT. The graphs show the absorption as functions of frequency when the cryostat is at rest (**a**) and when it is rotating at $\Omega = 1.21$ rad/sec (**b**). The lower graph in **b** shows a vertically expanded view of the satellite peak.[3] Figure 5

within the superfluid, but second-order transition lines should then emerge from the termination point. Experimentally none have been observed.

Flow of superfluid He^3

Persistent currents and frictionless flow are fundamental properties of a superfluid. Two methods have been employed for detecting persistent currents in superfluid He^3:

▶ By observing the persistent angular momentum of the fluid, using the gyroscopic principle: If superfluid circulates in a ring whose normal is in the z direction, a periodic torque about the x axis produces oscillations about the y axis with an amplitude proportional to the angular momentum of the circulating superfluid. Figure 7 is a photograph of the Cornell gyroscope.

▶ By measuring the flow-induced dissipation in a torsional oscillator. The motion of $\hat{l}$ dissipates energy through the so-called orbital viscosity; in an axial torsional oscillator this is proportional to $(v_s - v_n)^2$. A persistent current can thus be observed as a maximum in the Q value of the oscillator as a function of Ω (see figure 8). This method was devised at Cornell University for measurements[6] in He^3-A. It works also with He^3-B, but the theoretical framework is less secure.

The stability of persistent currents in He^3-B has been convincingly demonstrated both at Cornell and in a Helsinki–Berkeley collaboration: The observed[7] effective viscosity is at least 10^{12} times smaller than in the normal fluid. Persistent currents in He^3-A, on the other hand, apparently decay about 1% per day.

In our laboratory we measured[8] the critical value v_c for persistent currents in a torus of 22 mm major radius and 3 mm minor radius packed with plastic powder 20 μm in grain size to increase the critical velocity. We found a pressure-dependent discontinuity in v_c, with jumps of up to a factor of three. The jump occurs at a temperature close to the transition temperature T_v observed in nmr experiments on bulk liquid, and it too has been interpreted as originating from the vortex-core transition.

Mobility of negative ions

The soft vortex cores can be probed with measurements of ion mobility. A negative ion in liquid He^3 is a bubble of 1 nm radius containing one electron. In the A phase the ion moves in an external electric field $\mathbf{E}$ with the velocity

$$\mathbf{v} = -\mu_\perp \mathbf{E} + (\mu_\perp - \mu_\parallel)(\mathbf{E}\cdot\hat{l})\hat{l} \qquad (2)$$

where $\mu_\perp$ and $\mu_\parallel$ are the mobilities perpendicular and parallel to $\hat{l}$, respectively. Because the superfluid energy gap $\Delta(T)$ vanishes in the direction of $\hat{l}$ (see figure 3), there are more quasiparticles moving parallel to $\hat{l}$ than perpendicular to it; consequently, an ion experiences fewer collisions impeding its drift when it moves at right angles to $\hat{l}$. Typical values at a temperature of $0.8T_c$ are 0.12 cm^2/V sec for $\mu_\perp$ and 0.08 cm^2/V sec for $\mu_\parallel$.

The time of flight of an ion cloud through He^3-A depends on the $\hat{l}$ vector field, as equation 2 indicates; in an inhomogeneous texture different parts of the ion pulse travel with different velocities. In addition, typical textures in vortex structures focus ion trajectories into the core. Juha Simola and his coworkers at Helsinki have clearly observed[9] a drastic reduction in the velocities of negative ions when the superfluid is rotated, which demonstrates the strong focusing into regions with $\mathbf{v}$ along $\hat{l}$ caused by the vortex structures.

Very recent mobility measurements in He^3-A show also the presence of a vortex structure that does not induce a large change in the time of flight or in the shape of an injected ion pulse. This texture is obtained only after a slow, stepwise acceleration or after cooling under continuous rotation, and it is interpreted as a focusing singular vortex structure with large mobility along the core. The absence of this singular vortex type in the nmr experiments is attributed to the fact that ions may act as nucleation centers for singular vortices.

Vortex structures

The usual classification of vortices according to the circulation quantum number $K/(h/2m_3)$ is not sufficient for superfluid He^3. Because the order parameter has 18 degrees of freedom, there are several types of possible vortex structures for each value of the circulation number. Topological considerations are therefore used to classi-

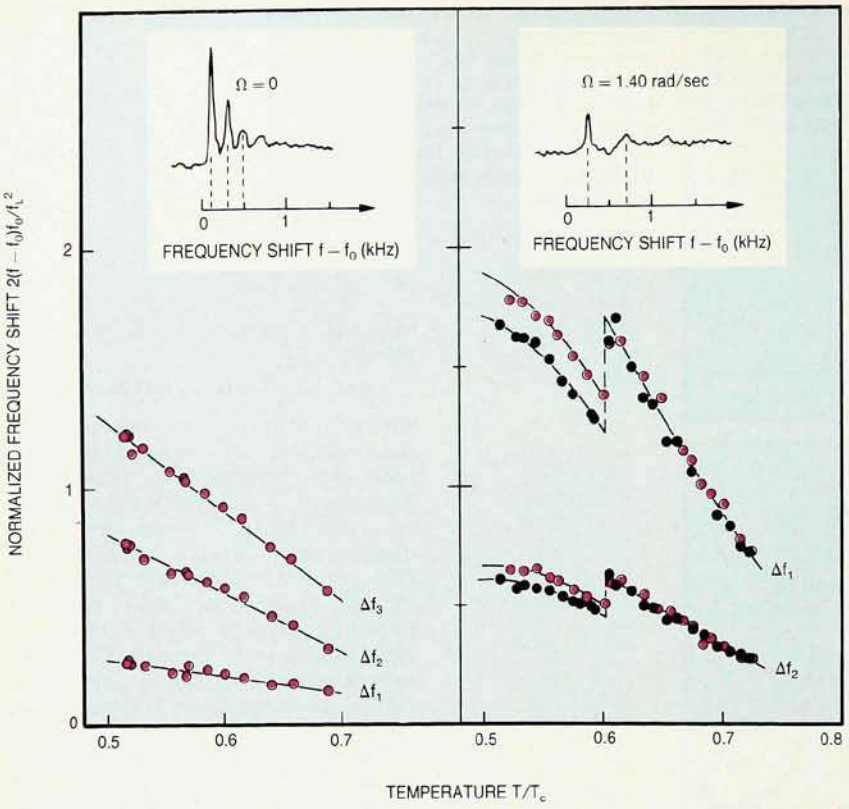

Frequency shifts as a function of temperature for the lowest three spin-wave resonance frequencies measured[5] in the stationary state (left) and the lowest two frequencies found during rotation at $\Omega = 1.40$ rad/sec (right). The colored dots refer to data taken for H parallel to Ω; the black dots, data for H antiparallel to Ω. The insets show experimental nmr spectra (at a temperature of $0.51T_c$). The frequency shifts are normalized to the (temperature-dependent) Leggett frequency f_L. Figure 6

fy vortex structures.[10] Martti Salomaa and Gregory Volovik[1] have developed a classification system based on the symmetries of the core structures. This scheme has greatly increased the understanding of vortices, and it has also helped to identify the vortex structures in rotating superfluid He^3.

The observed nmr satellite in He^3-A (figure 5) coincides[11] with that calculated for the nonaxisymmetric, doubly quantized vortex structure displayed in figure 9. There is no inversion symmetry in the core. As a result, the vortex core may exhibit spontaneous electric polarization and spontaneous axial superflow. However, other symmetries of the core may exclude either of these properties; in the vortex of figure 9, for example, electric polarization is prohibited.

Because of the intrinsic coupling between the spin and orbital parts of the He^3-A order parameter, it is possible to have vortices with a half-integer quantum of circulation.[12] In this case the vortex in the orbital space is combined with a singularity in the $\hat{d}$ field. The wavefunction must be single valued, so its phase may change only by $2\pi p$ upon circling a closed contour around a vortex. For $p = 1$, for example, the orbital and spin parts of the wavefunction can each suffer a change in phase of π during a full 2π rotation. The net effect for the total wavefunction Ψ is a change in phase of 2π; however, the vector $\hat{d}$ changes its sign, producing a disclination. The vortex is a half-quantum vortex with a circulation K of $h/4m_3$ along any path around the line defect.

The disclination in the $\hat{d}$ field acts as a starting point for a planar defect, which is costly in energy. To reduce the size of the defect, and thus the energy, two half-quantum vortices with opposite disclinations combine.[13] The size of the combined half-quantum vortices would be about 50 microns. These structures should appear in He^3-A between parallel plates separated by less than 10 microns when the temperature is below $0.5T_c$. Experimentally none have been found so far.

The core structure of a singular vortex in He^3-B is much more compli-

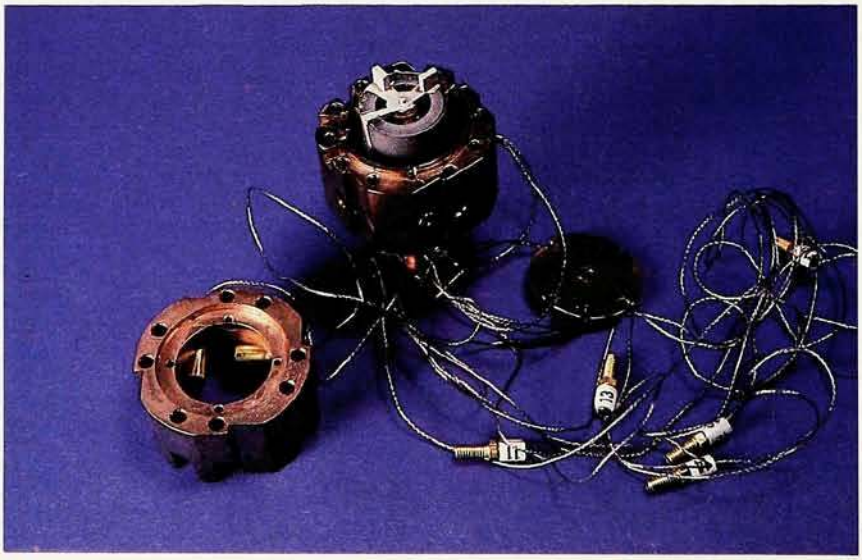

Gyroscope for observing persistent currents built by John Reppy and his coworkers at Cornell University. The gyroscope (partially disassembled here to show the sample cell) is used to observe persistent currents by measuring the response of the cell to a torque applied normal to the angular momentum of the circulating superfluid. (Courtesy of Peter Fraenkel.) Figure 7

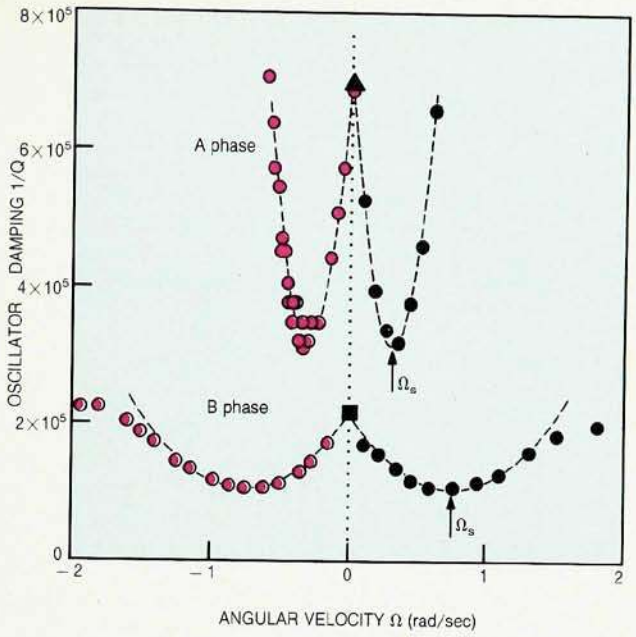

Damping, as measured by the inverse Q value of an axial torsional oscillator, as a function of the angular velocity of the cryostat.[6] The oscillator contains superfluid helium flowing in a ring 7 mm in mean radius and packed with 25-micron SiC powder. Torsional oscillations of the ring are damped least when the superfluid and the cryostat rotate at the same frequency Ω_c. The critical velocities, deduced from data measured at 29.3 bar, are 2.5 mm/sec for the A phase ($\rho_s/\rho = 0.10$) and 5.5 mm/sec for the B phase ($\rho_s/\rho = 0.93$). Figure 8

cated than that of a continuous vortex in He^3-A. The core of the B-phase vortex may involve all 18 components of the order parameter and thus its determination poses a difficult theoretical minimization problem.

Experimentally, one observes a change in vortex structures at the B1 to B2 phase transition. The key to this problem was first believed to be a profound change in the discrete symmetry properties of axisymmetric vortices; however, the currently favored explanation seems to be the breaking of axisymmetry.[14,15]

Minimizing the Ginzburg–Landau free energy at high pressures, one finds for the vortex core a nine-amplitude structure with axial symmetry. This structure contains superfluid phases in the core, which are responsible for the observed large spontaneous magnetic moment of the vortex cores in He^3-B. At lower pressures the free-energy minimization by Erkki Thuneberg[14] yields a complicated core structure with 180° rotation symmetry. The calculation displays a first-order transition between the nine-parameter core and the 180° rotation-symmetric core structures about 3 bars below the polycritical point, where He^3-A, He^3-B and the normal fluid coexist. This is in good agreement with experiments close to T_c.

Future prospects

In comparison with He^4, the superfluid phases of He^3 in rotation have been studied for only a short time. The nmr properties of rotating He^3-A and He^3-B have already been probed rather extensively. Their superflow and ion mobilities have been studied less thoroughly. Much still remains to be learned—for example, the A1 phase has not been investigated at all.

Several types of experiments appear promising for investigating rotating He^3, especially measurements involving zero sound—a collective oscillation in the distribution of quasiparticles on the Fermi surface. For superfluid He^3, the breakup of Cooper pairs leads to the appearance of absorption maxima. The absorption frequencies, which depend on the energy gap $\Delta(T)$, provide a means of studying inhomogeneous superfluid states. For example, in the A phase the attenuation of zero sound depends on the angle between $\hat{l}$ and the direction of zero-sound propagation.

In addition to providing data on individual vortex structures, nmr and zero-sound experiments are, in principle, capable of yielding information about the vortex lattice.[16] It may be possible to see absorption peaks due to Bragg reflections in zero sound. And it might even be possible to "photograph" the vortex lattice by using the focusing of negative ions by vortex cores in He^3-A; an analogous technique has been used on superfluid He^4.

Four types of vortices are already known in superfluid He^3—two in He^3-A and two in He^3-B—all different from the "classical" vortex of He^4. Theory says that many additional possibilities exist; several new phase transitions may thus be found, not only in the hard vortex core but also in the much more extended soft core. So far experimental studies of vortices in superfluid He^3 have concentrated on their static properties. In the future, one will be interested also in the dynamics of vortices: their nucleation, the mechanism of vortex-core transitions, and the formation of vortex rings. And what happens at the border region between the A and B phases?

Other fields may benefit as well from an improved understanding of vortex phenomena in rotating superfluid He^3. For example, the so-called heavy-fermion superconductors may also be based on Cooper pairs for which L and S are both 1. Half-quantum vortices are an example of topologically confined singularities. The singularity in the orbital part of the wavefunction is inseparable from the simultaneous singularity in the spin part. A pair of half-quantum vortices is "glued" together by a $\hat{d}$-vector string, and the force between the pair increases with separation. The situation is analogous to quark confinement.

A new cryostat, ROTA II, is under construction in Helsinki. This apparatus, which should become operational at about the time this article is published, incorporates many practical improvements over the old ROTA machine, both in refrigeration and in thermometry. For example, two charcoal pumps, working and regenerated alternately, allow continuous operation of the dilution refrigerator; this will increase the time available for experiments by a factor of three, at least. We hope that ROTA II will reach lower temperatures and turn six to eight times faster than the present cryostat, thus producing six to eight times as many vortices. The new apparatus will allow studies of He^3 in a high magnetic field, thus making vortices in

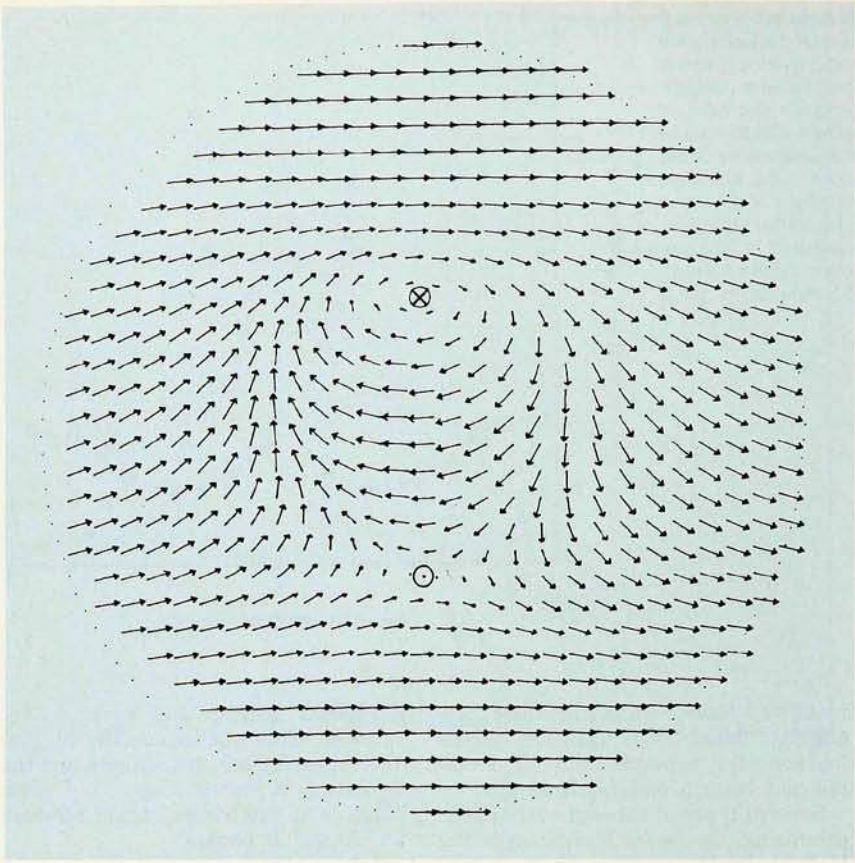

Vortex structure calculated[11] for He^3-A. This theoretically predicted continuous, doubly quantized, nonaxisymmetric structure is consistent with the experimental nmr observations. The arrows depict the projection of the $\hat{l}$ vector onto the plane perpendicular to Ω, which is directed out of the plane of paper. The points marked ⊙ and ⊗ denote positions where $\hat{l}$ is pointing parallel and antiparallel to Ω, respectively. According to equation 1 of the text, vorticity is concentrated into the region in which the $\hat{l}$ texture is nonuniform. Figure 9

He^3-A1 accessible.

Investigations of rotating superfluid He^3 have already shown that we are dealing with one of the most interesting systems in present-day condensed matter physics. While the third law prevents us from ever reaching 0 kelvin, low-temperature physicists have long since surpassed Nature herself, who has reached 3 K in the cosmic background radiation. Below the boiling point of He^3 we are thus creating physics hitherto unknown to the universe. And this has been done without any large expenditures of manpower or equipment—the most sophisticated tools at the cold frontier of physics are inexpensive indeed, by the standards currently in use in physics.

* * *

We are indebted to Alexander Fetter and Martti Salomaa for comments on the manuscript. This work was supported by the Academy of Finland.

References

1. G. E. Volovik, Usp. Fiz. Nauk. **143**, 73 (1984) [translation in Sov. Phys. Usp. **27**, 363 (1984)]. Yu. M. Bun'kov, G.E. Gurgenishvili, M. Krusius, G. A. Kharadze, Usp. Fiz. Nauk. **144**, 141 (1984) [translation in Sov. Phys. Usp. **27**, 731 (1984)]. V. P. Mineev, M. M. Salomaa, O. V. Lounasmaa, Nature **324**, 333 (1986). A. L. Fetter, in *Progress in Low Temperature Physics*, vol. 10, D. F. Brewer, ed., North Holland, New York (1986), p. 1. M. M. Salomaa, G. E. Volovik, Rev. Mod. Phys. (to be published in 1987). G. A. Kharadze, in *Modern Problems in Condensed Matter Physics*, W. P. Halperin, L. P. Pitaevskii, eds., to be published by North Holland, New York.
2. N. D. Mermin, Tin-Lun Ho, Phys. Rev. Lett. **36**, 594 (1976).
3. P. J. Hakonen, O. T. Ikkala, S. T. Islander, O. V. Lounasmaa, G. E. Volovik, J. Low Temp. Phys. **53**, 425 (1983). P. J. Hakonen, H. K. Seppälä, M. Krusius, J. Low Temp. Phys. **60**, 187 (1985).
4. A. J. Leggett, Rev. Mod. Phys. **47**, 331 (1975).
5. P. J. Hakonen, M. Krusius, M. M. Salomaa, J. T. Simola, Yu. M. Bunkov, V. P. Mineev, G. E. Volovik, Phys. Rev. Lett. **51**, 1362 (1983).
6. P. L. Gammel, Tin-Lun Ho, J. D. Reppy, Phys. Rev. Lett. **55**, 2708 (1985).
7. P. L. Gammel, H. E. Hall, J. D. Reppy, Phys. Rev. Lett. **52**, 121 (1984). J. P. Pekola, J. T. Simola, K. K. Nummila, O. V. Lounasmaa, R. E. Packard, Phys. Rev. Lett. **53**, 70 (1984). J. P. Pekola, J. T. Simola, J. Low Temp. Phys. **58**, 555 (1985).
8. J. P. Pekola, J. T. Simola, P. J. Hakonen, M. Krusius, O. V. Lounasmaa, K. K. Nummila, G. Mamniashvili, R. E. Packard, G. E. Volovik, Phys. Rev. Lett. **53**, 584 (1984).
9. J. T. Simola, K. K. Nummila, A. Hirai, J. S. Korhonen, W. Schoepe, L. Skrbek, Phys. Rev. Lett. **57**, 1923 (1986). J. T. Simola, L. Skrbek, K. K. Nummila, J. S. Korhonen, to be published.
10. N. D. Mermin, Rev. Mod. Phys. **51**, 591 (1979). V. P. Mineev, in *Soviet Scientific Reviews*, vol. 2, I. M. Khalatnikov, ed., Harwood, New York (1980), p. 173. M. Kléman, *Points, Lines, and Walls in Liquid Crystals, Magnetic Systems, and Various Ordered Media*, Wiley, New York (1983).
11. H. K. Seppälä, P. J. Hakonen, M. Krusius T. Ohmi, M. M. Salomaa, J. T. Simola, G. E. Volovik, Phys. Rev. Lett. **52**, 1802 (1984). X. Zotos, K. Maki, Phys. Rev. B **30**, 145 (1984). K. Maki, X. Zotos, Phys. Rev. B **31**, 177 (1985). V. Z. Vulovic, D. L. Stein, A. L. Fetter, Phys. Rev. B **29**, 6090 (1984).
12. G. E. Volovik, V. P. Mineev, Pis'ma Zh. Eksp. Teor. Fiz. **24**, 605 (1976) [translation in JETP Lett. **24**, 561 (1976)]. M. C. Cross, W. F. Brinkman, J. Low Temp. Phys. **27**, 683 (1977).
13. M. M. Salomaa, G. E. Volovik, Phys. Rev. Lett. **55**, 1184 (1985).
14. E. V. Thuneberg, Phys. Rev. Lett. **56**, 359 (1986).
15. M. M. Salomaa, G. E. Volovik, Phys. Rev. Lett. **56**, 363 (1986).
16. E. J. Yarmchuck, R. E. Packard, J. Low Temp. Phys. **46**, 479 (1982). □